

Structural, Vibrational and Molecular Docking Profiles of 3-Chloro -4-Methyl Anisole

C. Uma Devi^a B. Jayasutha^{a*}

^{a a*}P.G. & Research Department of Physics, H.H The Rajah's College(Affiliated to Bharathidasan University, Tiruchirappalli) Pudukkottai, Tamilnadu, India.

Article Info

Volume 83

Page Number: 176-197

Publication Issue:

September /October 2020

Abstract

The optimized molecular structure and corresponding vibrational assignments of 3chloro-4-methylanisole (CMA) have been investigated using Density Functional Theory (DFT)/B3LYP with 6-31 +G (d, p) and 6-311++G(d, p)basis sets. Making use of the recorded data, the complete vibrational assignments are made and analysis of the observed fundamental bands of molecule is carried out. The Mulliken charge analysis and the chemical reactivity and hardness of the molecule in terms of HOMO-LUMO energy gap have been implemented in terms of reactivity parameters. The MEP analysis was utilized for predicting the electrophilic and nucleophilic site in the CMA molecule. The biological activity of the CMA molecule were studied by using molecular docking analysis to identify hydrogen bond length and binding energies with different cancer protein. The CMA compound has been screened and found to exhibit anti-bacterial activity.

Article History

Article Received :04 June 2020

Revised: 18 July 2020

Accepted: 20 August 2020

Publication: 15 September 2020

INTRODUCTION

Anisole and its derivatives are used as a precursor for other synthetic compounds, solvents in perfumery; insect pheromones and pharmaceuticals [1-2].The functional groups

present in anisole lead to the variation of charge distribution in the molecule and consequently affect the structural, electronic and vibrational parameters. The enhanced nucleophilicity of anisole versus benzene reflects the influence of the methoxy group, which renders the ring more electron-rich[3].The heterocyclic compounds are those cyclic compounds whose ring contains one or more atoms of other elements besides carbon atoms. Because of the wide variety of physiological activities associated with the heterocyclic compounds, Many Anisole derivatives are well known for their high and diverse biological activities including antibacterial, antifungal, antiviral, pharmaceutical and agrochemical agents[4-5].The high electro negativity of halogens particularly (chlorine)in the aromatic part of the drug molecules plays an important role in enhancing their biological activity, This paper put forth the spectroscopic (FT-IR, FT-Raman,¹H NMR and ¹³C NMR)features and biological docking behaviours of methyl anisole derivatives. Furthermore, physicochemical properties and chemical reactivity of the molecules were defined based on the analysis of molecular electrostatic potential surface, non-covalent interactions and non-linear optical properties. Enzyme binding activity and docking behaviour of CMA were tested on a model enzyme structure of binding ligands. It is also possible to combine the spectroscopic and molecular docking analysis to identify the biological importance of methyl anisole derivatives. The DFT calculations were carried out by Gaussian 09 [6] and visualized with Gauss view programme. The molecule PED assignments,HOMO-LUMO,MEP and Mulliken charges were calculated through DFT studies.The pharmacological activity of a molecule depends on its geometric parameters and intermolecular interactions[7].

EXPERIMENTAL DETAILS

The sample of 3-Chloro-4-Methylanisole (CMA) is purchased from Sigma–Aldrich Chemicals, which is of spectroscopic grade and hence used for recording the spectra as such without any further purification. The FT-IR spectrum of the above compound is recorded in Bruker IFS 66V spectrometer in the range of 4000–400 cm^{-1} . The spectral resolution is $\pm 1 \text{ cm}^{-1}$. The FT-Raman spectrum of the above compound is recorded in Bruker IFS Raman module equipped with Nd: YAG laser source operating at 1.064 μm line width with 200 mW power. The FT-Raman spectrum is recorded in the range of 4000–100 cm^{-1} with a scanning speed of 30 $\text{cm}^{-1} \text{ min}^{-1}$ and spectral width 2 cm^{-1} . The frequencies of all sharp bands are accurate to $\pm 4 \text{ cm}^{-1}$.

QUANTUM CHEMICAL METHODS

The quantum mechanical calculations have been carried out by using the Gaussian 09W program package. The optimized structure and vibrational frequencies of CMA compound has been calculated by using DFT/B3LYP method with 6-311++G (d, p) basis set [8-9]. All computational calculations have been executed by adding polarization function d and diffuse function p on heavy atoms and also with triple split valence basis set for better reliable results. The Mulliken charge distribution of the present molecule is mapped and their values predict the pharmaceutical uses of the molecule. The electronic properties such as HOMO-LUMO analysis, global hardness, chemical potential, electro negativity have been used to elucidate information regarding charge transfer and chemical reactivity of the molecule. The auto dock program [10] was used for the molecular docking study.

RESULTS AND DISCUSSION

Structural analysis:

The molecular structure contains one benzene ring with chloro and methyl anisole. It was carried out using B3LYP/ 6-311++G(d,p) basis set, the parameters such as bond lengths and bond angles and dihedral angles are presented in the Table.1. The optimal picture of the structural compound is shown in Fig.1.

Table.1.

Optimized Geometrical parameters of 3-Chloro-4-Methylanisole using B3LYP/6-311++G (d, p) method and basis set

Bond length (Å)			Bond Angle (°)			Dihedral angle (°)		
C1-C2	1.395	1.395	C2-C1-C6	123.2	123.2	C2-C1-C6-C11	-180.0	-180.0
C1-C6	1.394	1.394	C2-C1-C115	117.19	117.1	C115-C1-C6-C5	-180.0	-180.0
C1-C115	1.766	1.766	C6-C1-C115	119.5	119.5	C115-C1-C6-11	-0.001	-0.001
C2-C3	1.395	1.395	C1-C2-C3	118.9	118.9	C1-C2-C3-C4	0.0007	0.0008
C2-H7	1.080	1.081	C1-C2-H7	119.1	119.1	C1-C2-C3-O10	-180.0	-180.0
C3-C4	1.398	1.398	C3-C2-H7	121.8	121.8	H7-C2-C3-C4	180.0	-179.9

C3-O10	1.363	1.363	C2-C3-C4	119.4	119.4	H7-C2-C3-O10	0.001	0.0014
C4-C5	1.385	1.385	C2-C3-O10	124.2	124.2	C2-C3-C4-C5	-0.0007	-0.0008
C4-H8	1.082	1.082	C4-C3-O10	116.2	116.2	C2-C3-C4-H8	179.9	179.9
C5-C6	1.403	1.403	C3-C4-C5	119.8	119.8	O10-C3-C4-C5	-180	-180
C5-H9	1.084	1.084	C3-C4-H8	118.8	118.8	O10-C3-C4-H8	-0.0003	-0.0003
C6-C11	1.506	1.506	C5-C4-H8	121.3	121.3	C2-C3-O10-16	0.001	0.002
O10-C16	1.421	1.421	C4-C5-C6	122.5	122.5	C4-C3-O10-16	-180	180.0
C11-H12	1.093	1.093	C4-C5-H9	118.9	118.9	C3-C4-C5-C6	-0.0001	-0.0002
C11-H13	1.093	1.093	C6-C5-H9	118.4	118.4	C3-C4-C5-H9	180.0	180.0
C11-H14	1.091	1.091	C1-C6-C5	115.8	115.8	H8-C4-C5-C6	180.0	-179.9
C16-H17	1.088	1.088	C1-C6-C11	122.8	122.8	H8-C4-C5-H9	0.001	0.001
C16-H18	1.095	1.095	C5-C6-C11	121.2	121.2	C4-C5-C6-C1	0.001	0.001
C16-H19	1.095	1.095	C3-O10-C16	118.6	118.6	C4-C5-C6-C11	-179.9	-179.9
			C6-C11-H12	111.5	111.5	H9-C5-C6-C1	-180	-180
			C6-C11-H13	111.5	111.5	H9-C5-C6-C11	0.001	0.0008
			C6-C11-H14	110.4	110.4	C1-C6-C11-12	-59.70	-59.6
			H12-C11-H13	106.8	106.8	C1-C6-C11-13	59.71	59.7
			H12-C11-H14	108.1	108.1	C1-C6-C11-14	180.0	180.0
			H13-C11-H14	108.1	108.1	C5-C6-C11-12	120.2	120.3
			O10-C16-H17	105.8	105.8	C5-C6-C11-13	-120.2	-120.2
			O10-C16-H18	111.3	111.3	C5-C6-C11-14	0.0026	0.004
			O10-C16-H19	111.3	111.3	C3-O10-C16-H17	180.0	-180
			H17-C16-H18	109.3	109.3	C3-O10-C16-H18	-61.2	-61.2
			C17-C16-	109.3	109.3	C3-O10-C16-H19	61.29	61.29

			H19		3		
--	--	--	-----	--	---	--	--

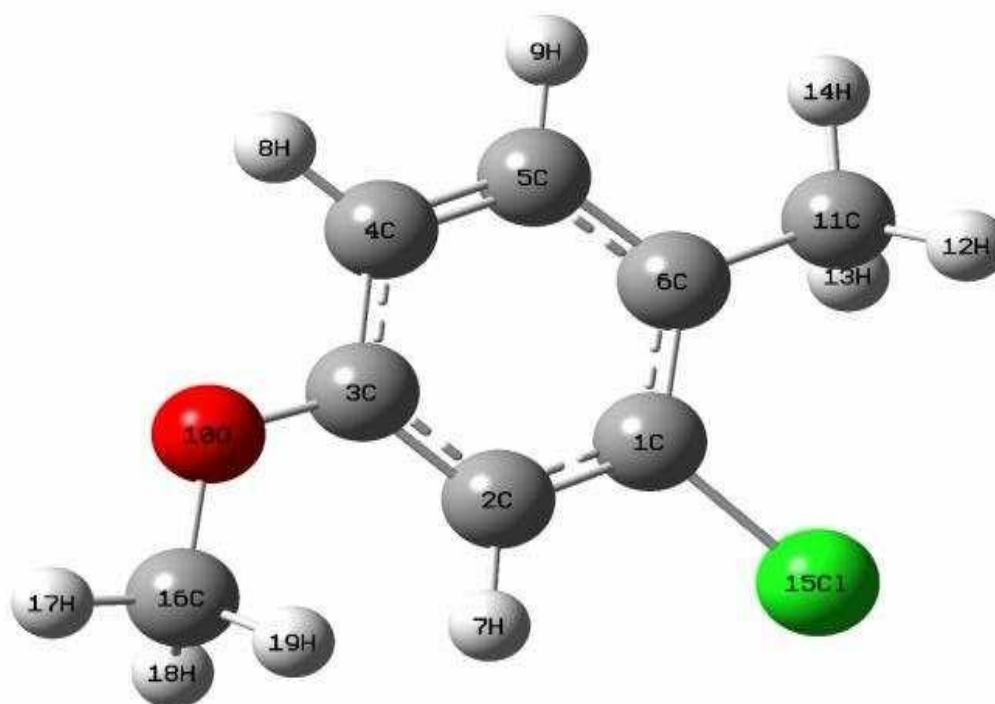


Fig .1 :Optimized molecular structure of 3-Chloro-4-Methylanisole with numbering scheme

The bond length for C-C single bond is expected to be around 1.45 Å and that of C-C double bond around 1.34 Å [11]. The bond length for C-C in the benzene ring is observed between 1.38 Å to 1.40 Å. This shows that the bonds present inside the benzene ring are neither double bond nor single bond and all the bonds have some intermediate values, which is in agreement with earlier work on benzene derivative [12], this may be due to the conjugation of the electrons inside the benzene ring which leads to almost equal distribution of electron density between the double and single bonds. The bond length for C5-C6 is observed to be 1.40Å. These slight increases in bond length may be due to the presence of the methyl group at C6 respectively. When the CO bonds in the molecule are compared, it is found that the O10-C16 bond length is 1.42 Å. This bond is present outside the ring, hence the influence on these bond lengths may not be significant. The C1-Cl15 bond length shows 1.76 Å. This shows that the bonds lie in the expected range.

Most elongated angles are C2-C1-C6 and C2-C3-O10 ranges are 123.2⁰ and 124.2⁰, the unevenness in the angle is mainly due to the uneven distribution of charges around the carbon atoms in the ring, which is influenced by the presence of oxygen atom inside the ring. The hybridization of these carbon atoms are greatly changed and hence the angles. Remains bond dihedral angles are uneven range due to the presence of O and Cl atoms. All the dihedral angles of the title compound are either nearly to 0 to 180⁰ which shows its planer nature.

The variation in bond angle depends on the electronegativity of the central atom, the presence of lone pair of electrons, and the conjugation of the double bonds. Bond order is a useful tool for characterizing bond type and measuring bond strength. The objective of the vibrational analysis is to obtain the vibrational modes connected with molecular structure of the compound under investigation. The harmonic vibrational analysis carried out for the optimized geometry.

Spectral analysis:

The vibrational assignments were done on the recorded FT-IR and FT-Raman spectra based on theoretically predicted wave numbers by DFT (B3LYP) level using 6-311+G(d,p) and 6-311++G(d,p) basis sets and are listed in Table.2 with their TED. Experimental Infrared and Raman spectra are shown in Fig.2 and Fig.3 respectively.

Table.2:

Vibrational assignments of experimental frequencies along with calculated frequencies of 3-chloro-4-methylanisole using B3LYP/6311++G(d, p) and B3LYP/ 6-311+G(d, p) basis set

S. No	Symmetry C1	Experimental Frequency(cm ⁻¹)		Theoretical Frequency				Assignment s with TED (%)
				B3LYP/ 6-311++G(d, p) cm ⁻¹		B3LYP/ 6-311+G(d, p) cm ⁻¹		
		FT-IR	FT-Raman	Unscaled	Scaled	Unscaled	Scaled	
1.	A	-	3180	3223	3184	3220	3178	v CH(98)
2.	A	-	3070	3197	3075	3192	3072	v CH(97)
3.	A	3060	-	3166	3066	3160	3064	v CH(98)
4.	A	-	3040	3135	3050	3130	3038	CH3ss(92)

5.	A	3002	3002	3107	3028	3100	3020	CH3ss(92)
6.	A	2951	-	3078	2960	3070	2955	CH3ips(94)
7.	A	-	2926	3064	2940	3060	2935	CH3ips(94)
8.	A	2836	2836	3029	2850	3024	2845	CH3ops(90)
9.	A	-	2820	3005	2830	2998	2825	CH3ops(90)
10.	A	-	1680	1647	1682	1640	1680	γ CC(88)
11.	A	-	1620	1600	1625	1596	1610	γ CC(88)
12.	A	1609	1609	1527	1611	1520	1598	γ CC(88)
13.	A	1578	1580	1505	1582	1500	1578	γ CC(89)
14.	A	-	1540	1495	1544	1491	1540	γ CC(88)
15.	A	1497	-	1492	1499	1490	1490	γ CC(88)
16.	A	1462	-	1482	1465	1476	1460	γ CC(89)
17.	A	-	1452	1472	1465	1467	1454	CH3ipb(83)
18.	A	1441	-	1424	1446	1420	1440	CH3sb(84)
19.	A	1382	1384	1418	1388	1415	1380	CH3sb(84)
20.	A	-	1320	1329	1325	1325	1320	b CH(70)
21.	A	1298	1298	1298	1300	1293	1295	γ CO(82)
22.	A	1280	-	1268	1285	1264	1282	b CH(70)
23.	A	-	1245	1228	1250	1220	1243	b CH(74)
24.	A	-	1210	1202	1212	1118	1205	b CH(74)
25.	A	1201	-	1167	1205	1166	1204	R trigd(72)
26.	A	1183	1184	1160	1185	1154	1185	R asym(70)
27.	A	-	1160	1062	1163	1055	1164	R symd(68)
28.	A	1151	-	1058	1154	1052	1153	b CC(72)
29.	A	1110	-	1052	1112	1045	1110	CH3opb(83)
30.	A	1047	-	1012	1050	1009	1045	CH3opb(83)
31.	A	-	1040	956	1044	950	1049	ω CH(56)

32.	A	995	-	890	999	885	992	ω CH(56)
33.	A	-	940	844	948	840	938	ω CH(56)
34.	A	877	878	823	880	815	875	b CO(54)
35.	A	840	-	751	842	750	838	CH3ipr(75)
36.	A	804	-	701	807	699	798	CH3ipr(75)
37.	A	744	743	693	748	690	746	ω CC(54)
38.	A	692	690	591	695	585	689	tRasym(72)
39.	A	660	-	540	664	535	662	tRsym(70)
40.	A	-	620	457	624	452	620	tRasym(71)
41.	A	587	-	454	590	450	585	γ CCl (86)
42.	A	552	-	434	555	432	549	CH3opr(76)
43.	A	-	540	352	544	345	539	CH3opr(76)
44.	A	-	474	334	477	330	470	ω CO(54)
45.	A	448	441	257	450	250	445	b CCl(64)
46.	A	-	343	242	347	241	343	tCH3(59)
47.	A	-	198	184	202	180	200	ω CCl (58)
48.	A	-	73	175	78	167	73	ν CH3(59)

Abbreviation: ν - stretching; b - bending; symd – symmetric deformation; asymd - asymmetric deformation; trigd- trigonal deformation; δ -out of plane bending; t– torsion; twist-twisting.

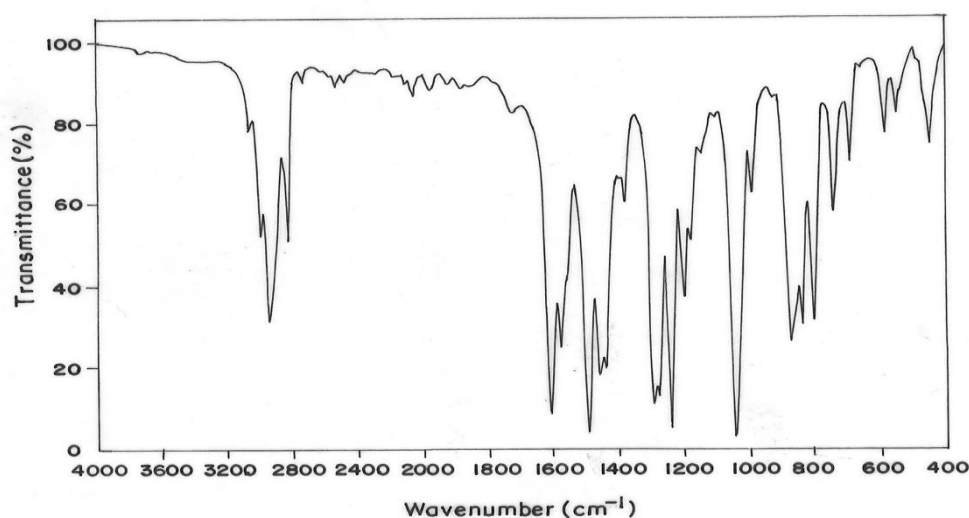


Fig.2 :FTIR spectrum of 3-Chloro-4-Methylanisole

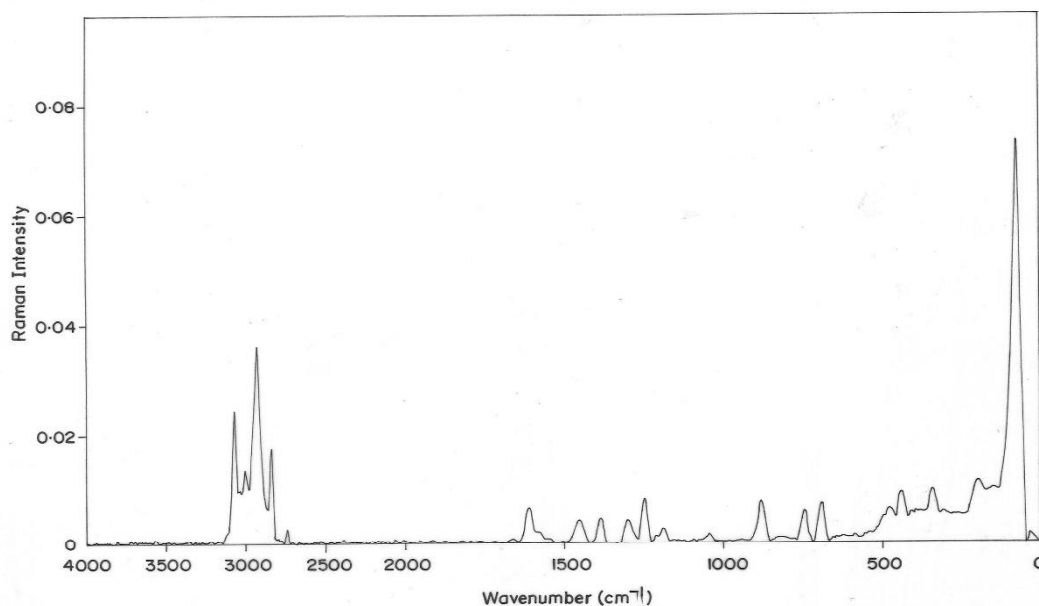


Fig .3 : FT-Raman spectrum of 3-Chloro-4-Methylanisole

The vibrational analysis obtained for CMA with the unscaled B3LYP/6-311+G(d,p) force field are generally greater than the experimental values due to neglect of anharmonicity in real system. Due to this reason, a discrepancy arises between observed and calculated vibrational wavenumbers in order to correct this, it is essential to scale down the theoretically calculated harmonic frequencies by introducing a scaled field or directly scaling the calculated wavenumbers with proper scale factor.

C-H Vibrations

Generally, all the aromatic C–H stretching vibrations of the benzene ring are normally expected between $3100\text{--}3000\text{ cm}^{-1}$ [13], which show the uniqueness of the skeletal vibrations. The present molecule CMA has three CH stretching vibrations. All three vibrations are found within the expected region, with values 3180 , 3070 , and 3060 cm^{-1} . All three bands are well within the expected range which confirms the fact that these are not affected by the substitution groups, as seen in previous analyses. All the modes are confirmed by their TED values.

Similarly, the C–H in-plane bending vibrations for aromatic molecule occur as strong to medium intensity bands in the region $1300\text{--}1000\text{ cm}^{-1}$ [14]. In the present case, the CH in-plane bending bands are observed at 1441 cm^{-1} in FT-IR and 1452 cm^{-1} in FT-Raman.

The calibrated values of CH bending vibrations are found at 1280, 1245, and 1210 cm^{-1} . Almost all the vibrations are found near the expected range. The C–H out-of-plane bending vibrations are expected in the region 1000–750 cm^{-1} [15]. The vibrations are found at 943-812 cm^{-1} in the present case. The experimental values, 1110 and 1047 cm^{-1} in FT-IR are exhibited. All these CH vibrations are found in the expected range and the vibrations of the functional group have not been affected by other vibrations.

CH₃ Vibrations

Methyl group attached along with methyl anisole and oxygen atom to a benzene ring. Methyl group vibrations are electron-donating substituents and can vibrate in different ways viz., CH₃ symmetric and asymmetric stretching, bending modes, and torsion. Methyl CH stretching mode appears at lower frequencies than those aromatic rings at 3000-2900 cm^{-1} . The anti-symmetric and symmetric deformations of the methyl group attributed in the region 1465-1440 cm^{-1} and 1040-900 cm^{-1} respectively [16]. The observed band of the CH₃ stretching is found in FT-IR at 3002 cm^{-1} and in FT-Raman at 3040 and 3002 cm^{-1} respectively. This model is confirmed by the TED value. The in-plane bending vibration is observed at 1441, 1382 cm^{-1} in FT-IR and 1452, 1384, 1320 in FT- Raman spectrum. The out-of-plane bending vibration is found at 812-583 cm^{-1} [17]. All these CH₃ vibrations are lying in the expected range which shows they are not affected by other modes.

C-C Vibrations

The C=C and C-C stretching vibrations present in benzene are usually assigned in the region 1600-1500 cm^{-1} and 1500-1400 cm^{-1} respectively [18], though they are not distinctly present inside the ring. In the present case, the CC single and double bonds are observed at 1609 and 1578 cm^{-1} in FT-IR respectively. The above conclusions are in very good agreement with the expected range. This is much important in the spectrum of the present molecule.

All the modes are confirmed by their TED values. The last two bands corresponding to CC single bond stretching are found to be relatively less, these are due to the mixing of the CH in-plane and CO stretching modes which also lie in this region. As an overall conclusion about CC vibrations, they are very well within the expected region hence they are not affected by the substitution groups, as CH skeletal vibrations.

C=O Vibrations

In this present investigation, the C=O stretching is obtained at 1298 cm^{-1} in both FTIR and FT-Raman spectrum. Hence, no such asymmetric and symmetric splitting is present in this molecule. The deformation mode of C=O is expected in the regions, 625 cm^{-1} and 540 cm^{-1} [19]. In this molecule, the deformation mode of C=O is represented in FT-IR having a value of 877 cm^{-1} and 878 cm^{-1} FT-Raman. Both the CO deformation mode and the bending CC mode of vibration are assigned the same value. All the modes are confirmed by their TED values.

C-Cl Vibrations

The title compound contains one Cl atom, which means it is capable to stimulate one C-Cl stretching vibration. The C-Cl vibrations are expected in the region of $850\text{-}550\text{ cm}^{-1}$ [20] and experimentally C-Cl vibrations are observed at 587 cm^{-1} . In stretching and bending regions are lies in the expected range.

Mulliken analysis:

Mulliken atomic charge calculations play an vital role in the application of quantum chemical calculations in molecular system. The atomic charges affects dipole moment, electronic structure and polarizability of the molecular system. The graphical representation of the total atomic charges of CMA were obtained by DFT with 6-311++G(d,p) basis set shown in Fig.4. In the present investigation, CMA have a benzene ring, its C_6 gets a maximum positive value of 0.764, and similarly C_3 also maximum negative range of -0.824.

If the charge distribution is also symmetrical within the benzene ring, all the carbon atoms within the benzene ring can also be equally negative, but the structural analysis revealed that there is no conjugation of electrons within the benzene ring, as they can share the electrons from the attached O atoms outside the ring [21]. The carbon atoms C1 (0.31), C8 (0.764) are positive. Considering the electron withdrawing capacity of the oxygen atoms relative to carbon and hydrogen, the charge predicted by Mulliken charge.

Table.3.

The Calculated Mulliken atomic charges of 3-Chloro-4-Methylanisole

Atoms	Mulliken charges (a.u.) B3LYP/6-311++G(d,p)
C1	0.317
C2	-0.447
C3	-0.824
C4	-0.142
C5	-0.454
C6	0.764
H7	0.195
H8	0.192
H9	0.131
O10	-0.154
C11	-0.811
H12	0.162
H13	0.162
H14	0.147
Cl15	0.606
C16	-0.336
H17	0.177
H18	0.156
H19	0.156

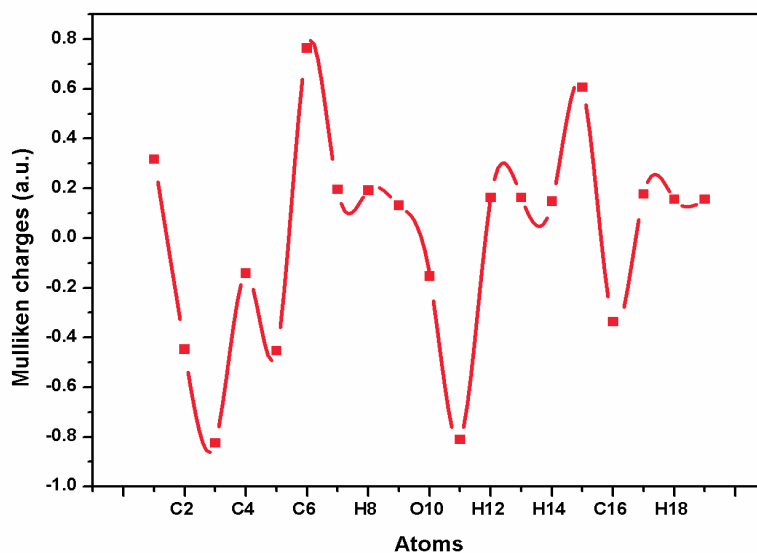


Fig.4 :The graphical representation of Mulliken charges for different atoms of 3-Chloro-4-Methylanisole

NMR analysis:

NMR spectroscopy has proved to be an exceptional tool to elucidate the structure and molecular conformations. To provide an explicit assignment and analysis of ^{13}C and ^1H NMR spectra, the theoretical chemical shift of the title compound is determined. The computational shifts were determined using gauge independent atomic orbitals (GIAO) functional along with B3LYP/6-311++G (2d,p) combination, the calculations were performed both in gas as well as in acetone solvent phases. The theoretical ^1H and ^{13}C NMR chemical shift values are presented in Table.4.and the corresponding spectra are presented in Fig.5 respectively. The phenyl carbon C1 atom is 148.4 ppm. It has the maximum chemical shift due to the attached Chlorine atom. The C11 and C16 are less deshielded 20.1 and 55.1 ppm. But these values are found higher than the literature where the values are methylare much shielded having values of 10 ppm [22]. In the case of the molecule, all the carbon atoms have almost the same shift between the range (113.9) to (165.3) ppm in the acetone method. The 3C atom has the maximum chemical shift of 165.3 ppm, the next value is 136.0 and 134.2 ppm for C5 and C6, which agrees with the high negative charge of these two atoms as discussed in the Mulliken analysis due to the presence of chlorine atom within the ring. Hydrogen atoms are almost localized on the periphery of the compound and their chemical shifts are not expected to be affected by the chemical environment [23], ^1H NMR chemical shift for H7, H8, H9 which are in the benzene ring are found to be 6.8, 6.9, 7.2 ppm. These are in the expected range for aromatic hydrogen. But the hydrogen in the methyl anisole group is expected in the range 3 to 4 ppm as they are in the aliphatic chain.

Table.4: The Calculated ^{13}C NMR and ^1H Chemical Shifts (ppm) for 3-Chloro-4-Methylanisole Computed at B3LYP/6-311++G(2d,p) GIAO

Atom	Gas	Acetone	Atom	Gas	Acetone
^{13}C Carbon			^1H Hydrogen		
1C	149.3	148.4	7H	6.6	6.8
2C	113.2	113.9	8H	6.8	6.9
3C	165.3	165.3	9H	7.0	7.2
4C	119.9	119.9	12H	2.3	2.3
5C	135.7	136.0	13H	2.3	2.3
6C	133.5	134.2	14H	1.8	2.0

11C	20.5	20.1	17H	3.9	4.0
16C	54.5	55.1	18H	3.5	3.6
			19H	3.5	3.6

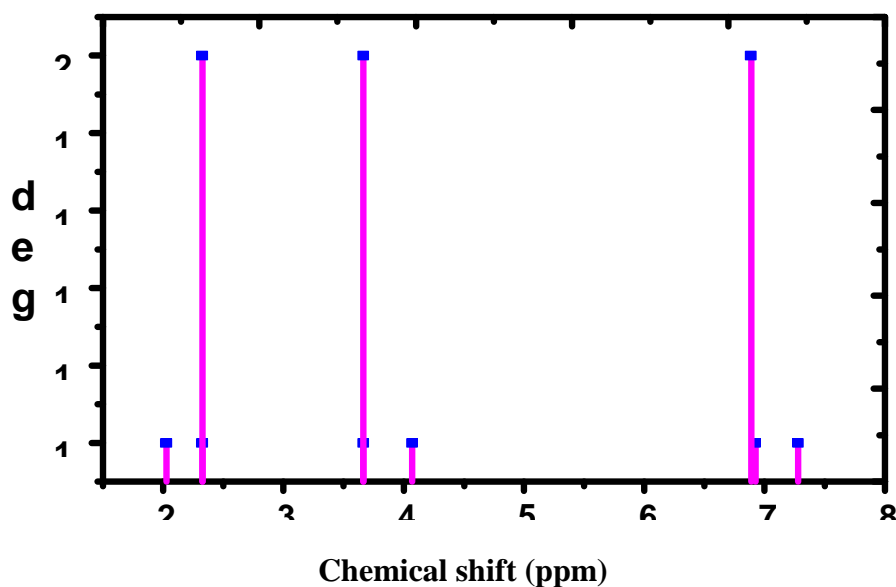


Fig. 5(a). ¹³C NMR Chemical Shifts (ppm) for 3-Chloro-4-Methylanisole

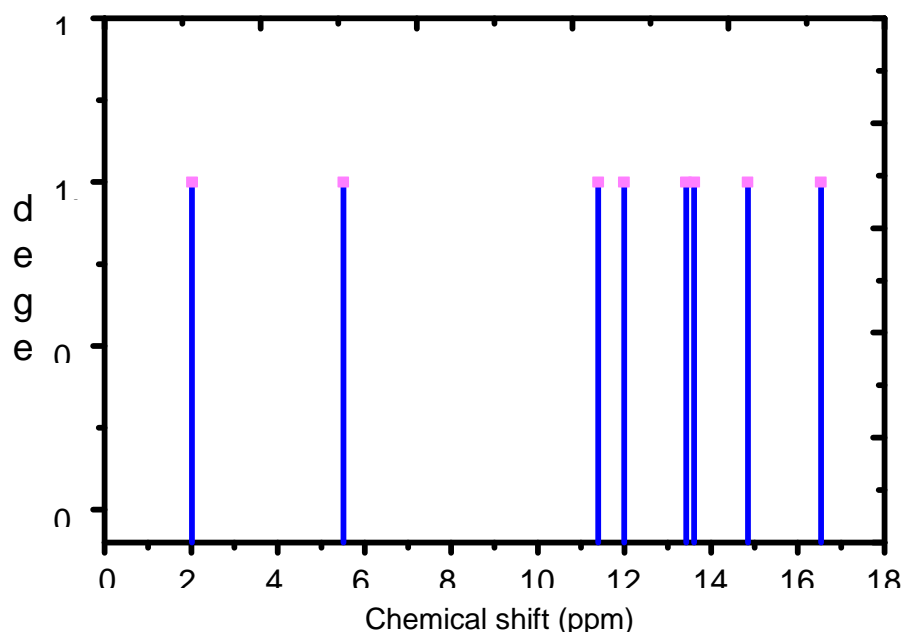


Fig. 5(b). ¹H Chemical Shifts (ppm) for 3-Chloro-4-Methylanisole

CHEMICAL REACTIVITY ANALYSIS

The properties which are evaluated using energies of HOMO and LUMO are the most essential in reactivity analysis, particularly in the spot of molecular synthesis and biomedical areas [24-25]. In this present investigation, the orbital energy gap (ΔE), HOMO and LUMO orbital energies and other important molecular reactivity parameters were evaluated by DFT/B3LYP 6-311++G(d,p) level and the corresponding results were reported in Table.5.

Generally, the energy difference of HOMO to LUMO is known as energy gap which elucidates the stability of molecular structure [26]. The global reactivity parameters of the title compound such as chemical potential, electro negativity, global hardness, softness and electrophilicity index can be determined by using HOMO and LUMO orbital energies of the molecule. These reactivity descriptors data of the present compound CMA can be evaluated by the following equations.

$$\text{Ionization potential } I = -E_{\text{HOMO}}$$

$$\text{Electron affinity } A = -E_{\text{LUMO}}$$

$$\text{Chemical potential } \mu = -\left(\frac{I+A}{2}\right)$$

$$\text{Global hardness } \eta = \left(\frac{I-A}{2}\right)$$

$$\text{Electro negativity } \chi = \left(\frac{I+A}{2}\right)$$

$$\text{Softness } S = \frac{1}{\eta}$$

$$\text{Global electrophilicity index } \omega = \frac{\mu^2}{2\eta}$$

As seen in Table.5, The ionization potential and electron affinity of the molecule indicate the ability to donate and accept electrons from neighboring molecular species. The chemical hardness (0.5687eV) indicating the molecule to be chemically stable. The electrophilicity index was found to be biologically active. Softness, another important descriptor predicts the toxicity of the chemical species. The title molecule has sufficiently softness value (0.8616 eV) suggest the molecule non-toxic nature theoretically [27].

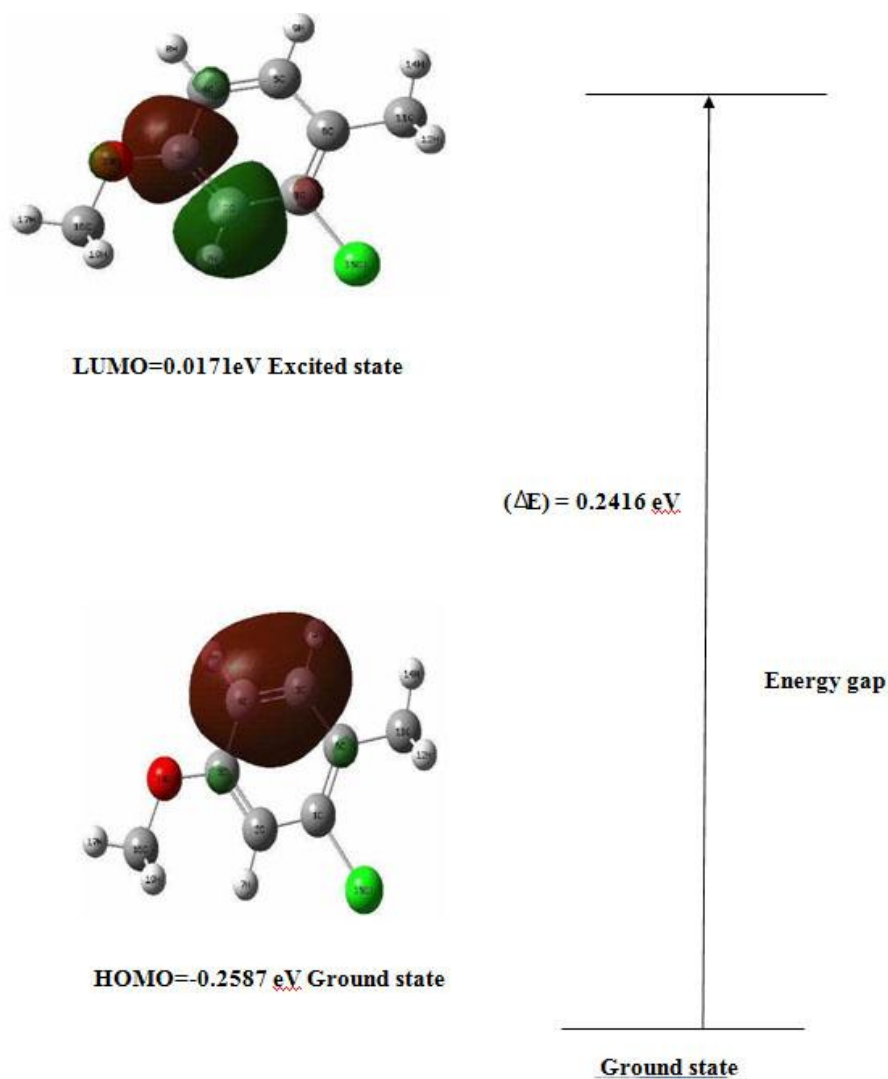


Fig.6. Pictorial representation of HOMO and LUMO for 3-Chloro-4Methylanisole

Table.5 :HOMO- LUMO energy values of 3-Chloro-4-Methylanisole

Parameters	Values
E_{HOMO} (ev)	-0.2587
E_{LUMO} (ev)	0.0171
$\Delta E_{\text{HOMO-LUMO gap}}$ (ev)	0.2758
Electro negativity (χ)	0.2929
Global hardness (η)	-0.5687
Global softness (S)	0.8616

Chemical potential	-1.4303
--------------------	---------

MOLECULAR ELECTROSTATIC POTENTIAL SURFACE

Molecular electrostatic potential is related to the electron density which is a very useful descriptor in understanding sites for nucleophilic reactions or electrophilic attack. As a result, this property was calculated for the target molecules at B3LYP/6-311++G(d,p) level of theory and indicated by a colour range from deep red to deep blue in the corresponding maps displayed. MEP was created by mapping of the electrostatic potential on the total electron density of the molecules for most active compounds shows in red the nucleophilic sites (negative potential) located at the oxygen atoms which result in hydrogen bond interaction[28]. The larger electrophilic sites (positive potential) appeared on the hydrogen attached to aromatic ring nitrogen consequence the blue cloud which was symbolized for electron deficient region, due to the accumulation of positive potential these moieties exhibited by hydrophobic interactions with the aromatic residues of active site in Fig.7. The MEP surface provides necessary information about the reactive sites.

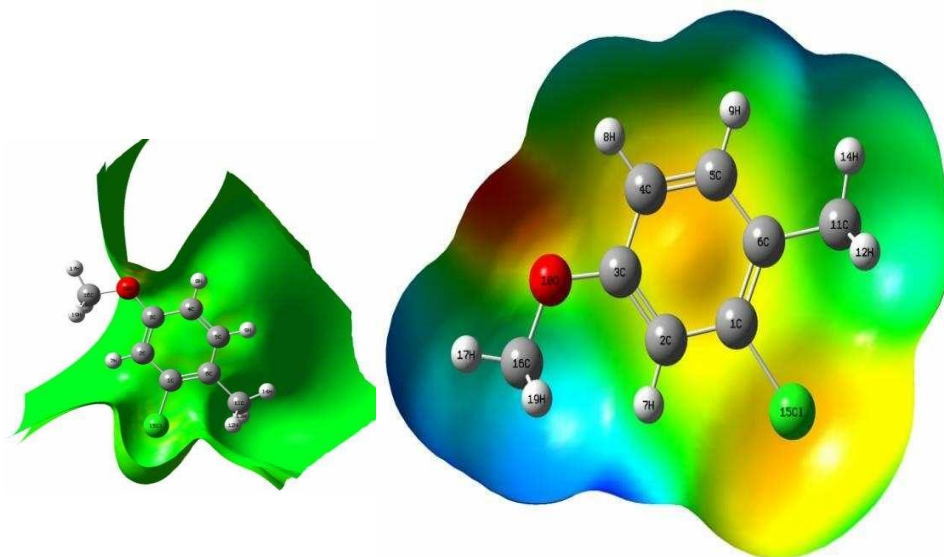


Fig. 7. Molecular electrostatic potential map for 3-Chloro-4-Methylanisole

MOLECULAR DOCKING ANALYSIS

Molecular docking is used to find the interaction between the ligand-protein. The pass (Predication of Activity Spectra for Substances) is an online tool to predict the activity of the CMA compound and also revealed that the compound have inhibitory activity. The residual structure of target is downloaded from RCSB (Research Collaboratory for Structural Bioinformatics) protein data bank .The Auto Dock Tools (ADT)graphical user interface has been used to prepare the protein by removing water and adding polar hydrogens along with charges [29-30].

The docking results shows that the aminoacids are LYS33:HZ3 forms a hydrogen bonds with a bond length of 1.8 Å. The protein 2WKF form a hydrogen bond with CMA ligand with binding energy 4.3 kcal/mol. The RMSD of the residue of the target protein to 1.36Åand it shows that the molecule has strong inhibitory activity.Fig.8 show the ligand – substrate interactions and Table.7. gives the binding affinity values of different poses of the title compound predicted by Autodock Vina.

Table: 7 The Calculated docking values for 3-Chloro-4-Methylanisole

S. No	Drug	Protein (PDB ID)	Docking score(k cal/mol)	H-Bond interaction	Distance(Å)
1	CMA	2WKF	4.3	LYS 33:HZ3 [O-H...O]	1.8

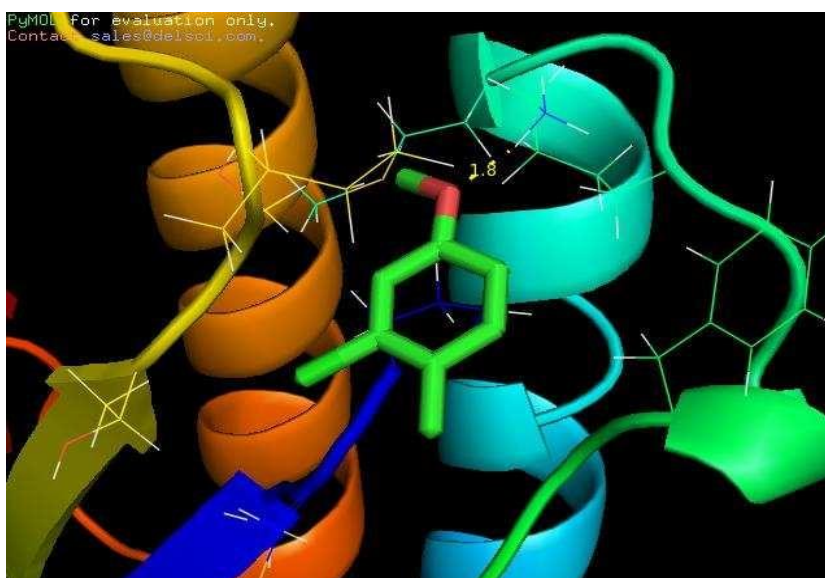


Fig.8. Docking pose for 3-Chloro-4-Methylanisole

ANTIMICROBIAL ACTIVITY

Agar disc diffusion method was used for the determination of antibacterial activity of the title compound CMA against two Gram-positive and two Gram-negative strains such as *Bacillus thuringiensis*, *Streptococcus aureus*, *Pseudomonas aureus* and *Echerichiacoli*[31]. The target bacterial strains were cultured in Mueller-Hinton broth (MHB). The title molecule CMA was dissolved in DMSO solution at concentration of 1 mg/ml. The concentrations of the tested molecule are fixed at 10 and 40 μ l. Amoxicillin was used as a positive standard reference to evaluate the sensitivity of each bacterial species tested. Antibacterial activity of tested compound was observed by measuring the diameter of the inhibition zone around the holes in each plate was measured and expressed in millimeters. The tested molecule displayed the highest inhibition efficiency (8-14mm) against all the bacterial strains when compared to standard antibiotic Amoxicillin. The electronic property of organic molecules is closely related to biological activity. The various substitutions of electron withdrawing atoms or groups such as fluoro, nitro and chloro on the benzene ring exhibited better biological activity. The observed zone of inhibition for antibacterial activity of CMA is shown in Table.8. From the observed results it is found that the title compound CMA showed greater activity against selected bacterial strains when compared to standard antibiotic[32-33].

Table:8 The Antibacterial activity of 3-chloro-4-methylanisole at different concentrations against bacterial pathogens;

S.No	Cultures	Diameter of the Zone of Inhibition in mm					
		10 μ l	20 μ l	30 μ l	40 μ l	Control	Antibiotic
1	<i>Bacillus thuringiensis</i>	14	12	11	10	Nil	16
2	<i>Staphylococcus aureus</i>	8	10	12	14	Nil	-
3	<i>Pseudomonas aureus</i>	-	8	10	12	Nil	-
4	<i>Echerichia coli</i>	-	-	-	-	Nil	17

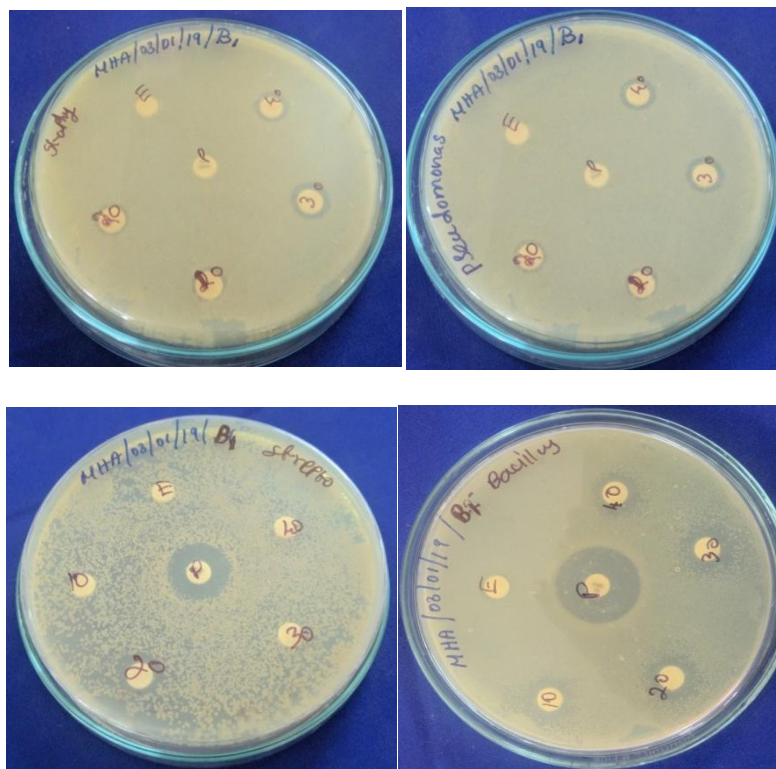


Fig.9 : Disk diffusion method of 3-chloro-4-methylanisole at different concentrations;

CONCLUSION:

A satisfactory vibrational analysis is made for CMA the present work. In this study, the vibrational frequencies were calculated and compared with the experimental data. It was found that the computations are in good agreement with experimental results. HOMO-LUMO energy gap explains the eventual charge transfer interactions taking place within the molecule. NMR study explains chemical shift of the title molecule. The reactive site of the title molecule has been found by MEP study. The molecular docking study shows that CMA molecule can bind with protein with binding energy of 4.3kcal/mol indicate the title molecules have pharmacological properties. *In vitro* antibacterial activity revealed that the title molecule CMA possess potent antibacterial activities toward bacterial strains and compared to standard drug Amoxicillin.

REFERENCES:

- [1] H.Fiege, H.W.Voges, T.Hamanmoto, S.Umenura, T.Iwata, H.Miki, Y.Fujitha, H.J.Buysch, D.Garbe, W.Paulus, phenol derivatives, Wiley, Weinheim-2002.
- [2] Etemkose, Journal of molecular structure (2020)129517.
- [3] M.Arivazhagan, N.K.Kandasamy, G.Thilagavathi Indian journal of pure and applied physics 50(2012)307.
- [4] P. Muniappan, R. Meenakshi, G. Rajavel, M. Arivazhagan, J. Spectrochim . Acta A 117 (2014)739.
- [5] Chiris.P, Muller, Michel.D, Collin Bach.D, Tan, Heather.A, Yogendra.P, Kharode and T.James.J.Med.Chem 44 (2001) 1654.
- [6] S.N.Pandeya, Alka Tyagi, Int.J.Pharmaceu.Sci, 3(2011) 53.
- [7] V. Krishnakumar, R. Ramasamy, Spectrochimica Acta Part A 61 (2005) 673.
- [8] **F.Jensen, "Introduction to Computational Chemistry", John Wiley & Sons, New York 1999.**
- [9] S.Kumaresan, V.Velmurugan, P.Palanisamy, N.Bhuvanesh, R.Subramanian, V.S.Pradosh and P.Ramkumar. Asian.J.Chem.Sciences (AJOCS) 2 (2017) 1
- [10] Anubha Srivastava, Rashmi Mishra, B.D. Joshi, Vineet Gupta & Poonam Tandon. Molecular Simulation, 40 (2014) 1099.
- [11] M.Gussoni, J. Mol. Struct. 141(1986)63.
- [12] M.Gussoni, C.Castiglioni, G.Zerbi, J.Chem.Phys.88(1984)600.
- [13] G.Socrates, Infrared and Raman characteristic Group Frequencies, third ed., Wiley, New York, 2001.
- [14] V.Krishnakumar, V.Balachandran, Spectrochim.Acta 63A (2006)464.
- [15] P.B.Nagabalasubramanian, M.Karaback, S.Periandy, Spectrochim.Acta A 85(2012)43.
- [16] D.N.Singh, I.D. Singh, R.A.Yadav, Ind.J.Phys.763(2002)307.
- [17] M.Karabacak, L.Sinha, O.Prasad, A.M.Asiri, M.Cinar, V.K.Shukla, Spectrochim. Acta A 123(2014)352.
- [18] V.Krishnakumar, R.John Xavier, Indian, J, Pure Appl. Phys.41(2003)95.
- [19] B.Venkkatram Reddy, G.Ramana Rao, Vib, spectroscosc, 6(1994)231.
- [20] Y.Sert, C.Cirak, F.Ucum, Spectrochim.Acta A 107(2013)248.
- [21] I.Sidir, Y.G.Sidir, M.Kumular, E.Tasal, J.Mol.struct, 964(2010)134.
- [22] M.Karaback, E.Kose, A.Atac, A.M.Asiri, M.kurt, J.Mol.Struct.1058(2014)79.

- [23] A.Ramamoorthy, C.H.Wu, S.J.Opella,J.Am.Chem.Soc 119(1997)10479.
- [24] I.Fleming,Frontier Orbitals and Organic Chemical Reactions, John Wiley and Sons, New York 1976.
- [25] S.SangeethaMargreat, S. Ramalingam, S. Sebastian, S. Xavier, S. Periandy, Joseph C. Daniel, M. Maria Julie, J.Mol.Struct 1200 (2020) 127099.
- [26] M. Arivazhagan, R. Kavitha, J.Mol.Struc 1011 (2012) 111.
- [27] V. Vidhya , A. Austine , M. Arivazhagan, Results in Materials 6 (2020) 100097, 1.
- [28] E.Scrocco,J.Tomasi,top,curr.Chem.42(1973)95.
- [29] A.Lagunin,A.Stepanchikova,D.Filimonov,V.Poroikov,Bioinformatics 16(2000)747.
- [30] O.Trott,A.J.Olson,J.comput.chem.31(2010)455.
- [31] V. Vidhya , A. Austine , M. Arivazhagan,Heliyon 6 (2020) e05464.
- [32] Thoraya A. Farghly, Magda A.Abdallah, Mohammed A.Khedr, Huda K.Mahmoud,J.Heterocyclic Chem 54 (2017) 2417.
- [33] Ajmal R.Bhat, Rajendra S Dongre, Pervaz A Ganie, Org and Med.Chem(2017) 1.